ingegneria sismica
International Journal of Earthquake Engineering
Anno XLIII - Num. 2 - 2026

Dynamic control of transmission and substation crane operations using digital twin and improved A* algorithm

Yi Zhou[1], *Haitao Jiang*[2], *Ming Song*[2], *Kangwei Li*[2] *and Hua Wen*[3,*]

[1] Beijing Power Transmission & Transformation Corporation, Beijing 102401 China
[2] State Grid Corporation of China's Ultra High Voltage Construction Branch, Beijing 102401 China
[3] Huada Tianyuan(Beijing) Science and Technology Co., Ltd., Beijing 102401 China

SUMMARY: *This paper first briefly introduces the application model of digital twin technology in crane operation, and then preprocesses the images taken during transmission and transformation crane operation using algorithms such as image enhancement and image edge detection, and detects and recognizes the operation of transmission and transformation cranes through an improved YOLOv5 model. After that, a raster map of point cloud data was drawn through the fusion of LiDAR and depth camera data, and an improved A* algorithm was proposed to realize the dynamic planning of transmission and substation crane operation by combining the operation characteristics of the transmission and substation crane hoisting equipment. The results show that the improved YOLOv5 algorithm has high detection accuracy and detection performance on the dataset. Meanwhile, the improved YOLOv5 target detection algorithm realizes the detection and determination of three types of violations with better detection accuracy. The improved A* algorithm significantly reduces the turning angle, the number of turns and the average number of search nodes by 77.19%, 40% and 39.2% compared with the traditional A* algorithm, which shortens the path planning time and the length of the planned path during the operation of the transmission and transformation crane. The improved A* algorithm is able to meet the global path planning requirements of the operation process of transmission and transformation cranes, and realize the dynamic control of the operation process of transmission and transformation cranes.*

KEYWORDS: *YOLOv5 model; digital twin technology; improved A* algorithm; transmission and substation crane operation*

1 Introduction

Currently, the demand for electricity in various countries is increasing day by day, and the construction of large-capacity, large-scale and smart grid has become the trend of power system development, and transmission and substation engineering projects are becoming more and more common, and the equipment that needs to be lifted and installed outdoors includes transformer ceramic bushings, disconnecting switch movable and static contacts, strut insulators, voltage equalizing rings, lightning arrester, current transformer, voltage transformer, and coupling capacitor equipment, etc. [1-4]. These equipments are generally arranged in the air of 2-3 meters, and the installation, maintenance and repair process requires the assistance of cranes. However, due to the narrow space of the transmission site, the small crane operation

*MK860303@163.com
https://doi.org/10.65102/is2026507
Published: 30 April, 2026

flexibility is insufficient, there is a “touch line” electrocution safety risk. The conventional treatment method needs to be blackout processing, the normal order of life and production of society will cause certain losses; in addition, the crane operator's operating safety knowledge is weak, the complex geological and hydrological conditions of the construction site, the operation of the equipment professionalism varies, equipment failure and other issues [5-8]. In view of this, transmission and substation crane operations need to have real-time, safety, economic realization of dynamic control.

Digital Twin (DT) is an inevitable product of digital transformation. Strategies such as Industry 4.0 promote the upgrade of physical systems from “static management” to “intelligent decision-making” - organizations need to grasp the operating status of equipment in real time to reduce downtime [9, 10]. Driven by this demand, the maturity of technologies such as the Internet of Things, artificial intelligence (AI), and cloud computing has provided a technical foundation for the "digital mirror image" of physical entities. It will shift from "static simulation of historical data" based on traditional simulation to "dynamic iterative real-time data" based on DT, in order to meet the intelligent management requirements of complex systems [11]. Lai et al [12] reported a shape-performance integrated DT technique to predict the structural performance of critical components and analyze the structure of non-critical components of crane equipment with the help of AI and analytical models based on sensor data, respectively, as well as to assess the safety of equipment operation for damage protection. Jiang et al [13] used a scaled model to design a DT framework with human-computer interaction to simulate and analyze the dynamic change patterns of different lifting behaviors on a tower crane as a means of assessing the stability of lifting safety, and to provide detection support for the risk of instability and the structure of the components in crane operations. Szpytko et al [14] constructed a DT conceptual model for integrated maintenance decision-making during crane operations, risk estimation and optimization through Markov chain Monte Carlo simulation model and particle swarm optimization algorithm in order to accomplish minimization of the risk and improve the efficiency of crane operations. Ma et al [15] proposed a dynamic collision risk warning system using AI-based target detection algorithms and stereo vision technology for feature capture and target 3D coordinate computation of each component in crane operations to realize high-precision safety supervision of substation crane operations. Zhidchenko et al [16] constructed a reference and simplified model based on dynamics and kinematics and used it to build a DT architecture for predicting real-time movements during crane operations to meet the operator's real-time management needs. Tu et al [17] proposed a DT-based mixed reality application interface for cranes to provide spatial registration and tracking for operators and to monitor crane status and manage crane movements under interactive holograms and bi-directional data communication, but only in a conceptual version. Hussain et al [18] constructed a DT framework for aging tower cranes, which predicts the ability of cranes to descend and ascend during operation through machine learning, and the DT framework charts the decline in load carrying capacity from 0-70 service life for a single crane, which assists in the load management of cranes in operation and improves the safety of operations. Yang et al [19] designed an industrial context-aware system based on DT and semantic technologies, which helps to cope with unexpected risks by real-time data integration and synchronization, as well as ontology-based environment modeling and augmented reality-based context-aware visualization for context-awareness and information management of dynamic environments in crane operations.

However, in power transmission scenarios, the application of DT technology in cranes still has difficulties, such as insufficient accuracy of the relevant prediction and detection models and insufficient efficacy of the optimal path design, which lead to collision and electrocution safety problems. The A* algorithm, as a search algorithm, plays a role in crane path planning

by finding the shortest path from the start point to the end point in the search graph. Farrage et al [20] used the A* algorithm for generating rotating crane motion trajectories for obstacle avoidance and load swing suppression, and optimizing the path time to achieve an optimal path under crane dynamics and load swing constraints. Bagheri et al [21] used the intelligent search advantage of the A* algorithm to provide a semi-optimal solution of the lifting sequence for multiple crane operations, which can minimize the idling time of the crane operations and thus reduce the crane operation cost and potential risks. Although the A* algorithm makes the classical path planning algorithm, the traditional A* algorithm has insufficient dynamic adaptability and is prone to searching for too many unnecessary nodes or omitting key reference factors thus falling into the trap of local optimization and approaching obstacles. Chu et al [22] used node labeling technique and incremental search node extension to improve A* algorithm so that it only identifies the critical nodes and modified the cost function to consider the distance cost of obstacles in the path optimal search to achieve safe and collision free path planning. Wang et al [23] reduced the number of critical nodes and the number of right-angle turns by adding extended distances to the traditional A* algorithm so that it retains extra distance from the obstacle QC, adding bidirectional search and smoothing for robust start and goal point path search. Niu et al [24] adapted the heuristic function of the traditional A* algorithm and introduced the dynamic window method and smoothing based on path optimization strategy to improve the planning efficiency and achieve real-time dynamic obstacle avoidance path planning. It can be seen that the targeted improvement of the A* algorithm and its combination with digital twin is expected to achieve dynamic control of transmission and transformation crane operations through virtual mapping, real-time data integration, simulation and derivation, and path planning optimization.

In this paper, digital twin technology is used to integrate the work content of transmission and substation cranes into the digital twin system, establish the overall application model of digital twin for crane hoisting process, and introduce the digital space, physical space and the connection between them in the model. After that, the collected picture samples of crane operation are preprocessed, and the pictures with complex backgrounds are binarized. Then an improved transmission and substation crane recognition model based on YOLOv5 is constructed, which classifies and recognizes the crane operation environment by introducing the Mish activation function and improving the Attention mechanism, and the SPP3 structure is utilized to increase the range of features received by the backbone network. Then the raster map is drawn from the collected point cloud data, and then the path of transmission and substation crane based on the improved A* algorithm is planned, and the performance of the recognition model and the application effect of the planned path are examined.

2 Crane operations management model using digital twins with improved A* algorithm

2.1 Application of digital twin technology in crane operations

2.1.1 Digital twin technology

Digital twin technology can effectively establish the connection between physical space and digital space. The assembly system guided by digital twin technology mainly consists of digital space, physical space and the link between the two. It specifically includes the following links:

1) According to the digital twin concept, the establishment of the digital twin assembly system of crane hoisting needs to formulate the hoisting process planning program based on the resource condition of the assembly site in the digital space, and adjust the production plan based

on the data feedback from the site to guide the lifting operation of the segments in the physical space when there are problems with the on-site assembly;

2) In the physical space, we need to do the preparatory work before lifting according to the planning documents of the lifting program of the segments formulated in the digital space, and at the same time, we need to execute the lifting process according to the planning results and guidance documents formulated in the digital space, collect all kinds of process data in the process of lifting site operation, and transfer the disturbing information to the digital space in a timely manner when encountering the unexpected situation;

3) Establishing an information feedback mechanism between digital space and physical space, which can ensure that the guidance documents in digital space are transmitted to the staff at the hoisting site, and can also categorize and feedback the construction records, completion conditions, testing results and other information at the hoisting site.

(1) Digital space

Segmental lifting program planning in the crane lifting process is mainly carried out in the digital space, according to the crane assembly process, the main work in the digital space for the segmental lifting sequence optimization, segmental lifting process simulation, the development of the segmental production design preparation program and the segmental lifting of the pre-preparation program and so on.

(2) Physical space

The main content of segment lifting in physical space is the physical assembly process in which each segment of the hull is transported to the crane and lifted and assembled in the crane. The assembly in the physical space is mainly based on the crane hoisting process guidance documents developed in the digital space.

(3) The connection between digital space and physical space

The connection between digital space and physical space is an important part of the digital twin, and the two-way flow of information between digital space and physical space is realized through the intermediate bridge of the hoisting database: in the whole process of planning the hoisting program to the hoisting of the crane on site, the digital space will transmit the process planning documents formulated to the database, and the staff of the hoisting in the physical space will check the planning guideline documents corresponding to the current operation state through the information terminal, and follow the guideline documents to ensure that the staff of the crane in the physical space will be able to carry out the assembly process according to the planning guideline documents. The lifting staff in the physical space will check the corresponding planning guidance document under the current operation status through the information terminal and carry out the lifting operation according to the guidance information.

2.1.2 Digital twin application model for crane operation process

To apply digital twin technology to the crane hoisting process, the first thing that needs to be done is to upload the factory's hoisting environment data, segment details, hoisting process requirements and other documents to the designated hoisting database, which is convenient for the staff to formulate and adjust the production plan. In the physical space, the lifting staff query the assembly guidance documents through the mobile terminal, complete the specified tasks according to the lifting process, and at the same time collect the information in the assembly process to provide basic data for the adjustment of the lifting program. The two-way circulation of data files between digital space and physical space is realized through the information transfer mechanism, which forms the digital twin application model of crane hoisting, and the dynamic control model of transmission and transformation crane operation is shown in Figure 1.

Based on this application model, after the crane lifting task is issued, the optimization

algorithm is used to optimize the lifting sequence of segments in the digital space, the lifting simulation is carried out on the segment model through the three-dimensional digital process design software to verify the reasonableness of the lifting sequence and the assembly process, and the reasonable process planning documents are formulated before the actual assembly and transferred to the information database through the information interaction system. At the actual lifting site, the personnel of the lifting team receives and learns the process guidance document through the mobile terminal, checks the segments and relevant lifting resources before lifting, and lifts the segments according to the lifting sequence obtained in the digital space, and scans the electronic tags of each segment during the lifting process to record the time point of lifting the segments and information of the personnel of the lifting team.

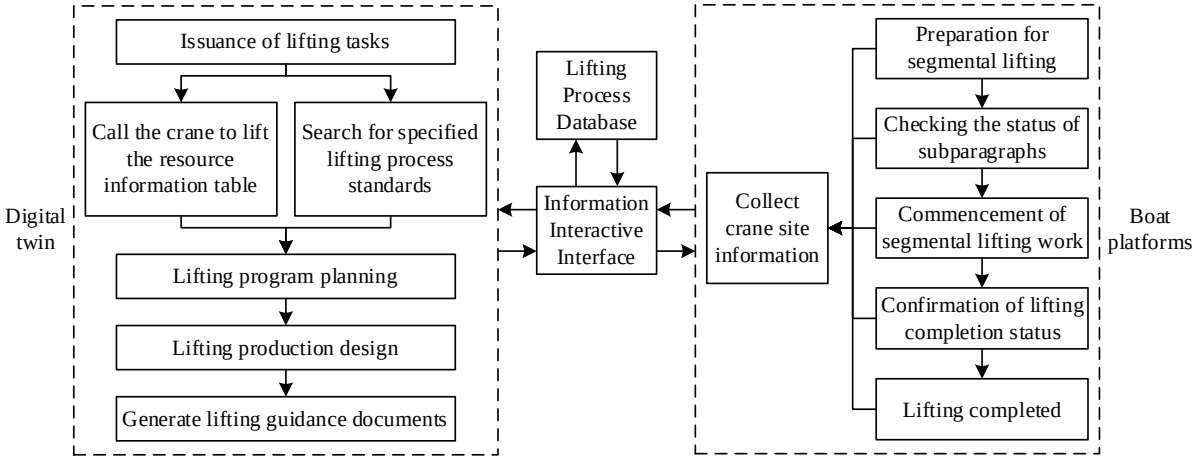

Figure 1: Operation Model of Crane for Power Transmission and Transformation

2.2 Environmental information recognition model construction for transmission crane operation

2.2.1 Image Preprocessing

Static image acquisition is mainly for the research of target recognition algorithm. The test images are selected to be taken during the operation of transmission and transformation crane in the natural environment of a factory in province J. The camera model is SONY A6400. The objects photographed in this paper are the crane, as well as the environment in which the crane is working, and the samples photographed are 1,000 images.

(1) Image Labeling

LabelImg is a dataset annotation software, which is often used for instance segmentation, semantic segmentation, target detection and classification in image annotation. In this paper, the following principles are followed in the annotation process:

1) If the crane operation process is shown completely in the image, all parts of the crane operation are boxed;

2) If the crane operation exists both near and far in the image, the near crane operation process is labeled;

3) If there are obstacles such as people and buildings in the image, both near and far, they are labeled.

(2) Image enhancement

Histogram equalization is a simple and effective image enhancement technique, which changes the grayscale of each pixel in the image by changing the histogram of the image, and

is mainly used to enhance the contrast of images with small dynamic range.

Suppose that a channel $f(x,y)$ of an image has a gray level of r and a gray level probability distribution of $p(s)$ after the following transformation:

$$s = T(r), \qquad 0 \le r \le L-1 \tag{1}$$

where L is the gray level and equal gray level probability distributions are obtained:

$$P_s(s) = \frac{1}{L-1} \tag{2}$$

The gray level distribution relationship before and after the transformation is:

$$P_s(s) = P_r(r)\frac{dr}{ds} \tag{3}$$

So get:

$$T'(r) = (L-1)p_r(r) \tag{4}$$

Points are obtained after:

$$s = T(r) = (L-1)\int_0^r p_r(w)dw \tag{5}$$

Expressed in terms of discretization:

$$s_k = (L-1)\sum_{j=0}^{k} p_r\left(r_j\right) = \frac{L-1}{MN}\sum_{j=0}^{k} n_j, \qquad k = 0,1,2,\ldots,L-1 \tag{6}$$

where k is denoted as the original image $p(r)$ quantized stratification.

(3) Image Edge Detection

Edge detection extracts key feature values in an image and is a low-level processing in image processing and computer vision. Common edge detection operators are Sobel operator, Laplacian operator and Canny operator.

1) Sobel operator

Sobel operator is a discrete difference operator which is mainly used to obtain the first order gradient of an image.Sobel operator is represented by the following equation:

$$\begin{aligned} S_x = &\{f(x+1,y-1) + 2f(x+1,y) + f(x+1,y+1)\} \\ &-\{f(x-1,y-1) + 2f(x-1,y) + f(x+1,y-1)\} \end{aligned} \tag{7}$$

$$\begin{aligned} S_y = &\{f(x-1,y+1) + 2f(x,y+1) + f(x+1,y+1)\} \\ &-\{f(x-1,y-1) + 2f(x,y-1) + f(x+1,y-1)\} \end{aligned} \tag{8}$$

2) Laplacian operator

The Laplacian operator is the simplest isotropic differential operator that is rotationally invariant. The Laplacian transform of a two-dimensional image function is an isotropic second-order derivative defined as:

$$f(x,y)=\frac{\partial^2 f}{\partial x^2}+\frac{\partial^2 f}{\partial y^2} \tag{9}$$

The discretization of the equation is expressed as:

$$\nabla^2 f=\{f(x+1,y)+f(x-1,y)+f(x,y+1)+f(x,y-1)-4f(x,y)\} \tag{10}$$

Degree values are preserved. The contrast of the pixels that make prominent changes in the gray scale is enhanced, highlighting the detailed information of the image.

3) Canny operator

Canny operator is based on the first-order differential operator detection algorithm and effectively suppresses the multi-response edges by adding non-maximum suppression and double threshold. It improves the edge localization accuracy of the image and reduces the leakage detection rate of the edges.

(4) Image Light Enhancement

For the images captured by the camera, the pixel value is not proportional to the brightness value of the object reflection. The camera response model is defined as:

$$P=f(E) \tag{11}$$

where E is the irradiance of the image, P is the pixel value of the image, and f should be satisfied:

$$F:=\{f \mid f(0)=0, f(1)=1, x>y\} \tag{12}$$

By comparing the histograms of two images with different exposure levels from the same from scene, it can be described by the following function:

$$P_1=g\left(P_0,k\right) \tag{13}$$

where P_1 and P_0 are images of the same scene with different exposure levels and k is the exposure ratio, the CRM is derived as:

$$g(f(E),k)=f(kE) \tag{14}$$

Retinex is an image enhancement algorithm that mimics the human visual system, based on Retinex theory there:

$$E=R\circ T \tag{15}$$

where R and T correspond to the reflection map and luminance map of the image respectively, take R as the image under ideal luminance, and substitute into the camera response model to obtain:

$$P=f(E), P'=f(R) \tag{16}$$

where P is the image of the actual that decomposition and P' is the image at the actual ideal brightness, then:

$$P' = f(R) = f(E \circ (1 \oslash T)) = g(f(E), 1 \oslash T) = g(P, 1 \oslash T) \tag{17}$$

The relation between T and k is obtained as:

$$k = 1 \oslash T \tag{18}$$

Let the initial luminance map be:

$$L(x) = \max_{c \in \{R,G,B\}} P_c(x) \tag{19}$$

The design weights are:

$$W_{d(x)} = \frac{1}{\left| \sum y \in \omega(x) \nabla dL(y) \right| + \epsilon}, d \in \{h, v\} \tag{20}$$

The objective function can be rewritten as:

$$\min_T \sum_x (T(x) - L(\mathrm{x}))^2 + \lambda \sum_{d \in \{h,v\}} \frac{W_{d(x)} (\nabla dT(\mathrm{x}))^2}{|\nabla dL(x)| + \epsilon} \tag{21}$$

Get the exposure ratio graph:

$$k(x) = \frac{1}{\max(T(x) + \epsilon)} \tag{22}$$

The final formula for the low brightness enhancement algorithm is obtained:

$$P'(x) = e^{b\left(1 - k(x)^a\right)} P_c(x)^{\left(k(x)^a\right)} \tag{23}$$

2.2.2 Transmission crane operation recognition model construction

(1) Activation function

①Mish activation function

When using YOLOv5 to train the dataset of transmission and transformation crane operation, it is found that the accuracy of the trained model is low, and a good activation function can enhance the model's representation and learning ability.The Mish activation function is smoother compared to the Leaky ReLu, which allows better information about the features of the crane operation to be passed through the neural network structure, thus strengthening the model's generalization ability and improving the model's accuracy. In YOLOv5, this paper adopts the Mish activation function, which constitutes the basic unit of this paper's model, CBM(Conv + BN+Mish), and the Mish activation function is:

$$Mish = x * \tanh\left(\ln\left(1 + e^x\right)\right) = x * \frac{e^{\ln\left(1+e^x\right)} - e^{-\ln\left(1+e^x\right)}}{e^{\ln\left(1+e^x\right)} + e^{-\ln\left(1+e^x\right)}} \tag{24}$$

②Hard-Mish activation function

In the Mish activation function, the $\tanh(x)$ function is a Sigmoid-type function with high

computational overhead, accordingly this paper optimizes the Mish activation function mathematically. The $\tanh(x)$ function is approximately linear in the middle region and saturated at both ends, so $\tanh(x)$ can be approximated by a segmented function. The first order Taylor expansion of the $\tanh(x)$ function near 0 is:

$$g_1(x) \approx \tanh(0) + x * \tanh(0) = x \tag{25}$$

Thus the $\tanh(x)$ function can be approximated by the segmented function $hard - \tanh(x)$, viz:

$$hard - \tanh(x) = \max\left(\min\left(g_t(x), 1\right), -1\right) \tag{26}$$

In the Mish activation function, $\tanh\left(\ln\left(1+e^x\right)\right)$ in e^x is greater than 0, and so $\ln\left(1+e^x\right)$ is transversely greater than 0. Then:

$$hard - Mish = \begin{cases} x * \ln\left(1+e^x\right) & 0 < \ln\left(1+e^x\right) \\ x & \ln\left(1+e^x\right) \geq 1 \end{cases} \tag{27}$$

(2) Attention mechanism

In order to enhance the model to pay more attention to the target area feature information in the transmission crane operation data set and weaken the background area information, the attention mechanism is introduced to let the model pay more attention to the flame and smoke area, so as to improve the accuracy of the model.

In this way the Attention mechanism can be viewed as each element in the output y vector is a weighted summation of the input x vector, and the weights are the importance of each element in the input x to each element in the output y. Each element in the input x can be seen as a series of <key, value> data pairs, and the weight coefficient can be seen as the correlation between each element Element in the output y and the key of each element in the input x, which can be obtained by learning based on a large number of samples in deep learning. Then the final Attention value is obtained by weighted summation of values, i.e.:

$$Attention(Element, x) = \sum_{i=1}^{len(x)} Similarity\left(Query, key_i\right) * value_i \tag{28}$$

The same c/r dimensionality reduction operation is used in the channel attention mechanism in CBAM. Combining the advantages of ECA module and the spatial attention mechanism in CBAM, this paper uses a two-way ECA structure for the channel attention mechanism and a CBM structure instead of conv for the spatial attention mechanism. The improved Attention machine is based on the schematic diagram of the channel domain, for the input feature map x , i.e:

$$Cout(x) = x * \sigma\left(CL_k(AvgPool(x)) + CL_K(MaxPool(x))\right) \tag{29}$$

where, $Cout\left(x\right)$ refers to the output of the channel domain attention mechanism in

ECA2_CBAM, the maximum pooling and the average pooling are done on the input x, and the pooled results are done as CL_k operations respectively, and CL_3 stands for Each pixel is convolved with the nearest three pixels in one dimension, and then the result of the convolution is summed up to do a sigmoid activation process, and the input x is multiplied with the value after activation to get the feature map with the information containing the channel's attention.

The spatial attention mechanism is mathematically expressed as:

$$Sout(x) = x * \sigma\left(f^{k*k}[Avg(x) \oplus \max(x)]\right) \tag{30}$$

where $Sout(x)$ refers to the output of the spatial-domain attention mechanism, $f^{k*}k$ denotes a convolution operation with a convolution kernel of size $k*k$, $\oplus$ stands for doing a splicing operation of the two-side feature maps in terms of their dimensionality, and σ is the sigmoid activation function.

The mathematical formula for the ECA2CBAM structure is:

$$E2Cout(x) = Cout(x) * \sigma\left(f^{k*k}[Avg(Cout(x)) \oplus \max(Cout(x))]\right) \tag{31}$$

For the input feature map x, the feature map containing spatial attention information and channel attention information will be output after ECA2_CBAM structure.

(3) Improvement of SPP

SPP3 first uses the standard CBM (Conv + BN + Mish) module to halve the input channels, then does a 3x3 average pooling, on top of the 3x3 average pooling do a 5x5 and 7x7 pooling respectively, in which each pooling process is used to fill means to keep the size of the feature map unchanged, the use of the average pooling can be avoided to avoid that a certain point of the information is too jittery and ignored the sampling zone Most of the numerical distribution, and finally the results of the three pooling and the data without pooling operation in the channel dimension are spliced together to do a CBM operation.

(4) General structure diagram of the model

After the above improvement, the final network model of this paper is now constructed. The improved model consists of four parts: Input, Backbone, Neck, and Prediction, and the improvement and role of each part are as follows:

1) Input: this stage includes preprocessing the dataset, adjusting the size of the predefined anchor frame, utilizing the Mixup method to increase the samples of the occlusion scene, utilizing the Mosaic method to increase the samples of the small target data, and adjusting the processed Transmission Crane operation dataset to a size of 640x640 to send it to the Backbone stage.

2) Backbone: This stage is mainly used to extract image features on different scales, using smoother Mish activation function to replace the original Leaky Relu activation function, adding the improved Attention structure SE_CBAM after the CSP1_X structure, and replacing the original SPP with the improved SPP3.

3) Neck: this stage is for better feature extraction and multi-scale fusion of different scales of features extracted by Backbone.

4) Prediction: this stage is the prediction stage, which outputs three feature maps of different sizes for predicting the target in the image.

2.2.3 Point cloud data for map construction

(1) Estimation of crane position

When constructing the map, firstly, the position of the crane in the map should be confirmed,

and then the relative position of the crane operation should be obtained by LiDAR and Real Sense D455 camera, so as to indirectly obtain the position information of the crane operation on the map. There are two main methods for the positioning of transmission cranes:

1) Odometer localization

The photoelectric encoder and inertial measurement unit are used to measure the translation speed, rotation angular speed and other information of the transmission crane in real time, and the data fusion is carried out through the EKF algorithm, and then the position information of the transmission crane is derived through the trajectory projection.

2) Scanning matching localization

Laser scanning matching localization is to realize localization by calculating the relative position transformation between the fused laser scanning data and the map, and launching the displacement of the transmission crane relative to the previous moment.

(2) Drawing raster map

In this paper, the crane operation information jointly calibrated by LiDAR and Real Sense D455 camera is finally transformed into LiDAR scanning data format, which is used to construct a 2D raster map of the environment.

(3) Lidar and depth camera data fusion

Since the data collected by LiDAR only contains environmental information on one horizontal plane, and the depth image collected by D455 contains multiple horizontal planes, it is necessary to perform data fusion between the two.

Assuming the current need to convert the mth column of pixel points, all the pixels in this column will be converted into a virtual LIDAR point, and the distance of the laser point is:

$$d_K = \min\left\{r_K(n)\right\} s \le n \le s+h \tag{32}$$

$$r_K(n) = \left|AO_K\right| = \sqrt{s_k^2 + x_k^2} \tag{33}$$

where S denotes the wheel radius height, h denotes the transmission crane height, and $r_K(n)$ denotes the distance from the D455 camera origin O_K to the virtual LIDAR point, which is angled:

$$\beta = \arctan\left(x_K \Big/ z_K\right) \tag{34}$$

Let the set of LiDAR scanning data (r,α) be D_L, and after fusing the $P'(u,v)$ coordinate data and depth information Z_k collected by the D455 camera, the set of the new scanning data is obtained as D_F, P is the i th crane in D_L. operation point, the LiDAR scanning data is $\left(d_i^L, \alpha\right)$, and the derivation leads to the coordinates of P under $\left(O_K, X_K, Y_K, Z_K\right)$:

$$\begin{bmatrix} x_K \\ y_K \\ z_K \end{bmatrix} = \begin{bmatrix} R & T \\ 0^T & 1 \end{bmatrix} \begin{bmatrix} d_i^L \sin\alpha \\ l \\ d_i^L \cos\alpha \end{bmatrix} \tag{35}$$

The virtual LiDAR ranging data d_i^K corresponding to P can be obtained. The obstacle

is detected in the same direction, and the fused i th beam LiDAR scanning data $\left(d_i^F, \alpha\right)$ is:

$$d_i^F = \begin{cases} d_i^k & d_i^K < d_i^L \\ d_i^L & \text{Other} \end{cases} \tag{36}$$

When both LIDAR and D455 are working at the same time, the data are continuously collected and fused according to the above method, and the fused scanning data set D_F is obtained. Since the measurement angle β range of the LiDAR is larger than the measurement angle α of the D455 camera, i.e. $\left[\beta_{\min}, \beta_{\max}\right] \subset \left[\alpha_{\min}, \alpha_{\max}\right]$, the scan data set D_F of the fusion result is obtained as:

$$\begin{aligned} D_F = & \left\{ d_i^F | i \in \frac{\left[0, \beta_{\max} - \beta_{\min}\right]}{\Delta\beta} \right\} \cup \{ d_i^L \mid i \notin \left[0, \frac{\left(\beta_{\max} - \beta_{\min}\right)}{\Delta\beta} \right] \text{ and} \\ & i \in \left[0, \frac{\left(\alpha_{\max} - \alpha_{\min}\right)}{\Delta\alpha} \right] \end{aligned} \tag{37}$$

where $\Delta\alpha$ denotes the angular increment of the lidar and $\Delta\beta$ denotes the angular increment of the virtual laser of the D455 camera. So far, the data fusion of LiDAR and depth camera has been completed.

2.3 Transmission crane operation path planning based on improved A* algorithm

2.3.1 Transmission Crane Lifting Equipment Path Planning Modeling

(1) Overview of environmental modeling of transmission and substation crane rigging equipment

Establishing an accurate spatial model or map is the purpose of environmental modeling, which describes the spatial location of various objects in the working environment of transmission and substation crane hoisting equipment, such as obstacles and road signs.

(2) Raster method to create an environmental map

The raster map refers to the decomposition of the entire environment into many discrete rasters, each of which is assigned a value representing whether or not the raster is occupied by an obstacle. Constructing a map of the environment for a transmission and substation crane hoisting equipment requires coding the map to indicate whether or not an obstacle is present at a particular raster location, and the simplest way to do this is to use the binary numbers 0 and 1. If there is an obstacle at that location, it is encoded using 1 and the free raster is encoded with 0. The raster map can then be equated to a binary map.

(3) Raster map processing based on transmission and substation crane hoisting equipment

In order to establish a mathematical model of the transmission and substation crane hoisting equipment, the following assumptions need to be used:

1) Assume that the transmission and substation crane hoisting equipment works in a two-dimensional plane space, excluding the lifting and lowering of the hook of the transmission and substation crane hoisting equipment in the vertical direction, i.e., keeping the hook rope length unchanged during the movement of the transmission and substation crane's large and small vehicles.

2) Simplify the dimensions of the hook in the crane, and use a point to characterize the position of the transmission and substation crane hoisting equipment.

3) Assume that the location of obstacles in the environment of the transmission and substation crane lifting equipment are known.

4) In order to improve the safety of the operation of the transmission and substation crane hoisting equipment, the path of travel of the transmission and substation crane hoisting equipment should not be in contact with the boundary of the obstacle, i.e., it is better not to take a diagonal route.

(4) Transmission and substation crane lifting equipment path planning search rules

When using ACO algorithm for path planning, it is necessary to search the raster in the environment map, and the mainstream raster map search algorithm has eight directions of search and four directions of search. In this paper, the raster method is used for modeling, if the eight-direction search is used, the planning path will go diagonal, i.e., there is a possibility that the planning path will be adjacent to the obstacle raster, and there is a possibility that it will collide with the obstacle when the hook load is swinging.

2.3.2 Improved A* Algorithm Path Planning Principles

(1) Principle of A* algorithm path planning

As an extension of Dijkstra's algorithm, A* algorithm is a kind of heuristic search algorithm.A* algorithm, as a typical representative of heuristic search algorithms, is widely used in the shortest path solving problem of mobile robots.A* algorithm can be said to be an optimal search algorithm.

The formula of A* algorithm is:

$$f(n) = g(n) + h(n) \tag{38}$$

where $f(n)$ denotes the cost estimation function from the starting point to the goal point via the current state point n; $g(n)$ denotes the actual cost from the starting point to the current state point n; and $h(n)$ denotes the heuristic estimation cost from the current state point n to the goal point. In this equation, let the heuristic function $h(n) = \left|x_n - x_{goal}\right| + \left|y_n - y_{goal}\right|$.

(2) Improved A* algorithm path planning principle

When the traditional A* path planning algorithm is used for the path planning of transmission and transformation crane lifting equipment, the resulting path will produce many turning points, which may lead to an increase in the number of starts and stops of the transmission and transformation crane motor, the lifting of goods to reduce the efficiency of the load swing increase and other issues. Let the improved A* algorithm be formulated as:

$$f(n) = g(n) + h(n) + \varphi(n) \tag{39}$$

where $\varphi(n)$ denotes the cost of the equipment lifted by the transmission and transformation crane during its movement.

Order:

$$\varphi(n) = \begin{cases} k * h(n), & \text{Turning angle of } 90° \\ 0, & \text{Turning angle of } 180° \\ k * h(n), & \text{Turning angle of } 270° \end{cases} \tag{40}$$

where k is the number between $(0,1)$, the specific size depends on the actual situation. It can be seen that adding a new heuristic function $\varphi(n)$ can make the transmission and transformation crane lifting equipment path planning process as much as possible to take a straight line and reduce the turning points. It can be seen that this improved algorithm is a comprehensive optimization between the shortest path and the least turning points.

2.3.3 Planning Steps for Improved A* Algorithm Paths

Let S be the starting point and E be the goal point, the path planning search algorithm is to start with S and then search for each neighboring point of S. The search continues sequentially until the goal point E is searched. The steps to improve the A* algorithm are as follows:

(1) Initially, first simplify the load of transmission and transformation crane lifting equipment to a point and establish a two-dimensional raster map.

(2) Add the start point S to the open list of the raster. The rasters in this open list are the rasters to be searched.

(3) Find all points adjacent to the start point S that are not occupied by obstacles and add them to the open list of the raster.

(4) Remove the start point S from the open list of the raster and add it to the closed list of the raster. The rasters in the closed list will no longer participate in subsequent searches.

(5) Select a neighboring raster in the open list of rasters, and the raster with the lowest improved f value will be selected. By continuously repeating the process of searching for the raster with the lowest improved f-value, the combined optimal path in terms of path length and number of turning points can be generated.

3 Dynamic operation simulation analysis of transmission crane operation

3.1 Behavioral detection results of transmission crane operations

3.1.1 Experimental environment

In this paper, we chose an Intel i9 9900K processor for the hardware, a 24G memory NVIDIA Titan RTX for the graphics card, and two 16G memory sticks to form a dual-channel; Ubuntu 18.04.6 operating system was installed on the software, the computing framework of the graphics card was CUDA 10.2, and the deep learning framework used was PyTorch 1.6. 0. In addition to this, for data processing and model training, third-party libraries such as Pandas, Numpy, OpenCV, and Matplotlib were used. The datasets are all used as 70% as training set, 10% as validation set and 20% as testing set. Based on the above experimental environment and homemade dataset size, batch_size is set to 16 and epoch is 120 during training.

3.1.2 Target detection

The field-photographed dataset of people standing under the lifting boom and lifting boom operators leaving their posts is put into several classical target detection models and the improved YOLOv5 model in this paper for training and evaluation, and the test results of the different methods are shown in Table 1.The SSD acquires less raw image data to begin with than that of the other networks, as well as a relatively weaker feature learning capability, and performs the worst on this dataset, with a mAP of only 0.8076, but its performance is faster than that of YOLOv3 and YOLOv4. The YOLO series is getting stronger and stronger in terms of detection accuracy and performance during the iteration process of the versions, and the

enhancement is especially obvious between YOLOv3 and YOLOv4, where the mAP improves by 0.049 on this dataset while the time consumed stays almost the same as the original.

The size of the input image of YOLOv5 increases from the original 256×256 to 640×640, which retains more information about the original image and saves computational cost in the inference process, and a lot of improvements have been made on the basis of YOLOv4, so the improvement of the detection accuracy and performance is very considerable. In this paper, we replace the Mish activation function which is more adaptable to the dataset on the basis of YOLOv5, and at the same time, we add the SE_CBAM structure after each CSP1_X structure in the backbone, and the mAP of the improved YOLOv5 on this dataset reaches 0.9932, and the final detection performance is about 60 frames, which can satisfy the requirement of real-time detection.

Table 1: Test results of different methods

Network	SSD	YOLOv3	YOLOv4	YOLOv5	Improved YOLOv5
Input size	256×256	300×300	412×412	620×620	640×640
mAP	0.8076	0.8133	0.9289	0.9308	0.9932
Time (s)	0.0201	0.0298	0.0168	0.0163	0.0141

The safety sign dataset taken in the field and the safety sign dataset generated by the improved Attention mechanism are put into several classical target detection models and the improved model in this paper for training and evaluation, and the test results on the safety sign dataset are shown in Table 2. For YOLOv5, the detection accuracy is higher than that of the previous generations of YOLO even when the dataset is not augmented with data from the improved Attention mechanism. When the dataset is enhanced with the improved Attention mechanism data enhancement, the mAP value is improved from 0.9655 to 0.9701. And the mAP value of the improved YOLOv5 on the dataset enhanced with the improved Attention mechanism data enhancement reaches the highest value of 0.9878, which shows that the use of the data enhancement with the improved Attention mechanism can make multiple networks with different degrees of accuracy enhancement.

Table 2: Test Results on Safety Sign Data Set

Network	SSD		YOLOv3	YOLOv4	YOLOv5		Improved YOLOv5	
Input size	256×256		300×300	412×412	620×620		640×640	
Perspective collineation	No	Yes	No	Yes	No	Yes	No	Yes
mAP	0.7301	0.7862	0.9131	0.9409	0.9655	0.9701	0.9715	0.9878

In this paper, when the improved YOLOv5 is trained on the lifting crane boom under stander and lifting crane boom operator off duty dataset, the lifting crane boom operator off duty dataset performance is shown in Figure 2. As can be seen from the figure, the detection accuracy of this model for the operator reaches 0.9702, for the relatively small number of lifting cranes, lifting booms and cockpits reach more than 98%, the more obvious features of the boom is 0.9954. This model achieves better results between the categories, which can be seen that the detection model has a good adaptability for this task.

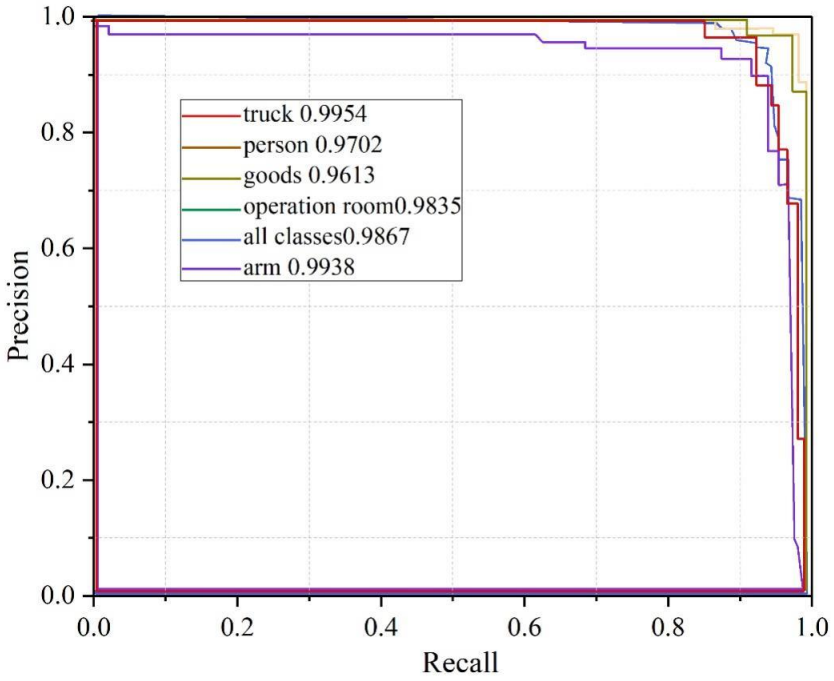

Figure 2: Performance of crane boom operator off-duty data set

The performance of the improved YOLOv5 in this paper when trained on the safety sign dataset enhanced by the improved Attention mechanism is shown in Figure 3 below. From the figure, it can be seen that the detection accuracy of this model for signage and all types of safety signs reaches 0.9827, of which signage, prohibited signs, instruction signs and prompt signs even reaches 0.9954.This model achieves better results among all types, which shows that the detection model is also well adapted for this task.

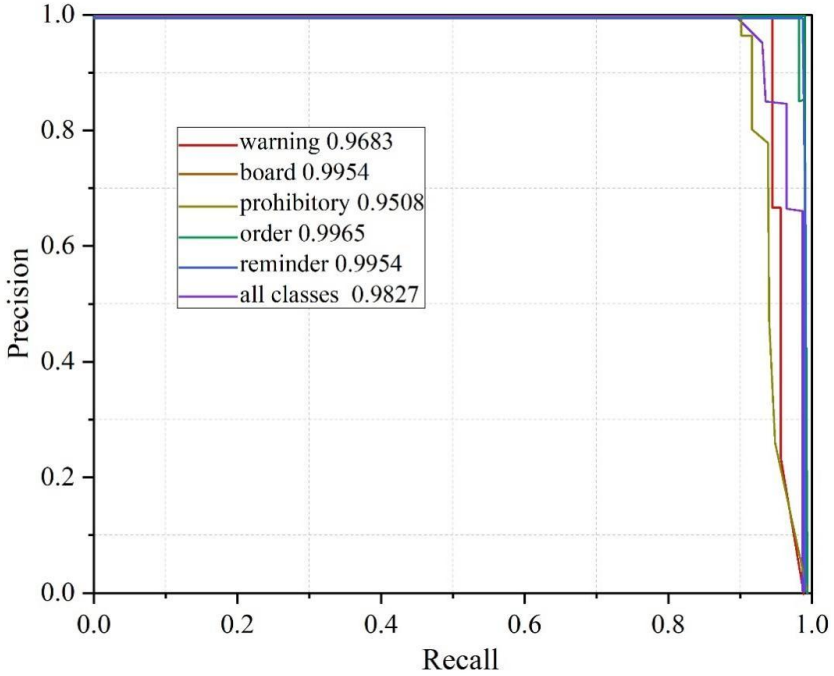

Figure 3: Perspective Transformation Enhanced Safety Sign Data Set

3.1.3 Determination of violations

Based on the detection results of the improved YOLOv5 network model, this paper proposes different detection algorithms for the three types of violations, such as people standing under the lifting boom, lifting boom operators leaving their posts, and missing safety signs, to realize the detection of violations in the lifting operations at construction sites, and the final detection rate on the homemade dataset is shown in Table 3. The average detection rate of the scene modeling-based detection method proposed for the violation of standing under the lifting boom in the three scenes of the homemade dataset is 88.10%, due to the fact that the operators in the homemade dataset are smaller, the detection rate of the method is mainly affected by the detection accuracy of the operator and the target of the lifting boom in the screen; the detection rate of the target-tracking-based detection method proposed for the violation of the lifting boom operator leaving the workplace is 88% in the three scenes of the homemade dataset. The average detection rate of the proposed region-based detection method for the violation of missing safety signs is 93.11% in the three scenes of the homemade dataset, due to the fact that the safety signs in the homemade dataset are smaller and farther away from the camera, but the target tracking method is used; the average detection rate of the proposed region-based detection method for the violation of missing safety signs is 93.11% in the three scenes of the homemade dataset, due to the fact that the safety signs in the homemade dataset are smaller, but with a moderate distance from the camera. But with moderate distance from the camera, and the crane is a large target in the screen, so the detection rate of the method is mainly affected by the detection accuracy of the safety signs and crane in the screen.

Table 3: Detection rate on self-generated datasets

Irregularities	Person standing under the crane boom (%)	The crane boom operator is absent from the post (%)	Safety sign missing (%)
Scenario 1	87.53	92.94	93.53
Scenario 2	88.31	91.75	92.68
Scenario 3	88.46	90.29	93.12
Mean	88.10	91.66	93.11

3.2 Transmission crane operation path planning

3.2.1 Simulation test of improved A* algorithm

To validate the performance of the proposed path planning algorithm for crane operations, the simulation experiments are conducted in MATLAB 2022b environment. The algorithm simulation tests are conducted in a 36 m × 36 m raster map. The test will be the improved algorithm of this paper and the traditional A* algorithm in the constructed raster map environment for 8 times path planning simulation test, the simulation results are obtained. The performance comparison results of traditional A* algorithm and improved A* algorithm are shown in Fig. 4 and Fig. 5, respectively. The algorithm performance comparison results are shown in Table 4. The simulation results show that the improved A* algorithm reduces the turn angle by 77.19%, the number of turns by 40% and the average number of search nodes by 39.2% on average. This indicates that the improved algorithm runs faster, generates smoother paths, and is able to plan global paths in a shorter time.

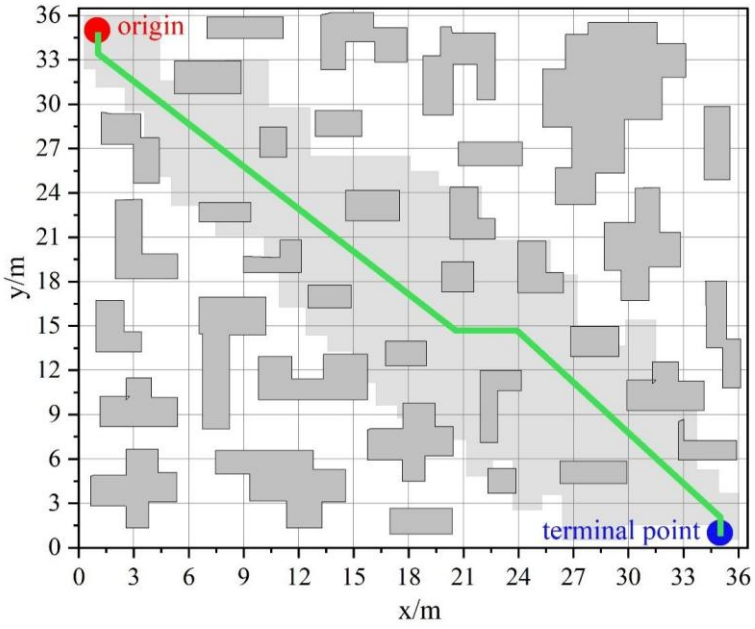

Figure 4: Traditional A algorithm*

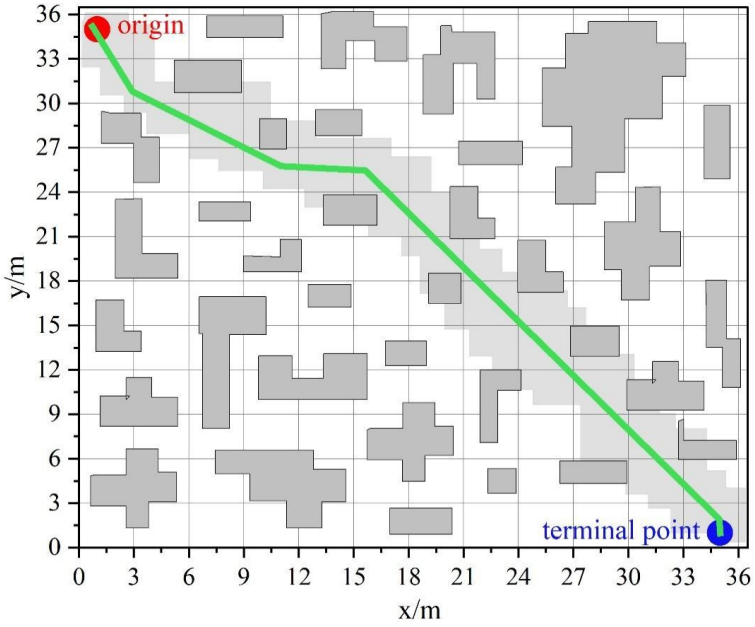

Figure 5: Comparison of Performance of Improved A Algorithm*

Table 4: Algorithm performance comparison results

Algorithm performance	Traditional A* algorithm	Improved A* algorithm
Average turning angle (°)	263	60
Average number of turns (times)	5	3
Average search node count (items)	125	76

3.2.2 Simulation test of improved A* algorithm

To verify the performance of the proposed improved A* algorithm, simulation tests are conducted in a dynamic obstacle environment. The fusion algorithm aims to solve the path planning problem from the starting point to the goal point, adding dynamic and static obstacles

in the static raster map, the dashed line is static planning, and the solid line is dynamic planning, the results of the dynamic obstacle avoidance path planning are shown in Fig. 6, in which (a) is the start of obstacle avoidance for dynamic 1, (b) dynamic 2 passes through the dynamic obstacles, (c) dynamic 3 passes through the static obstacles, and (d) dynamic 4 reaches the goal point. As can be seen from the figure, the fusion algorithm successfully avoids the added obstacles and achieves a smooth angle and a smaller turning angle of the planned path. Based on the planning results in Fig. Linear velocity, angular velocity and attitude angle of the dynamic control of transmission crane operation are plotted.

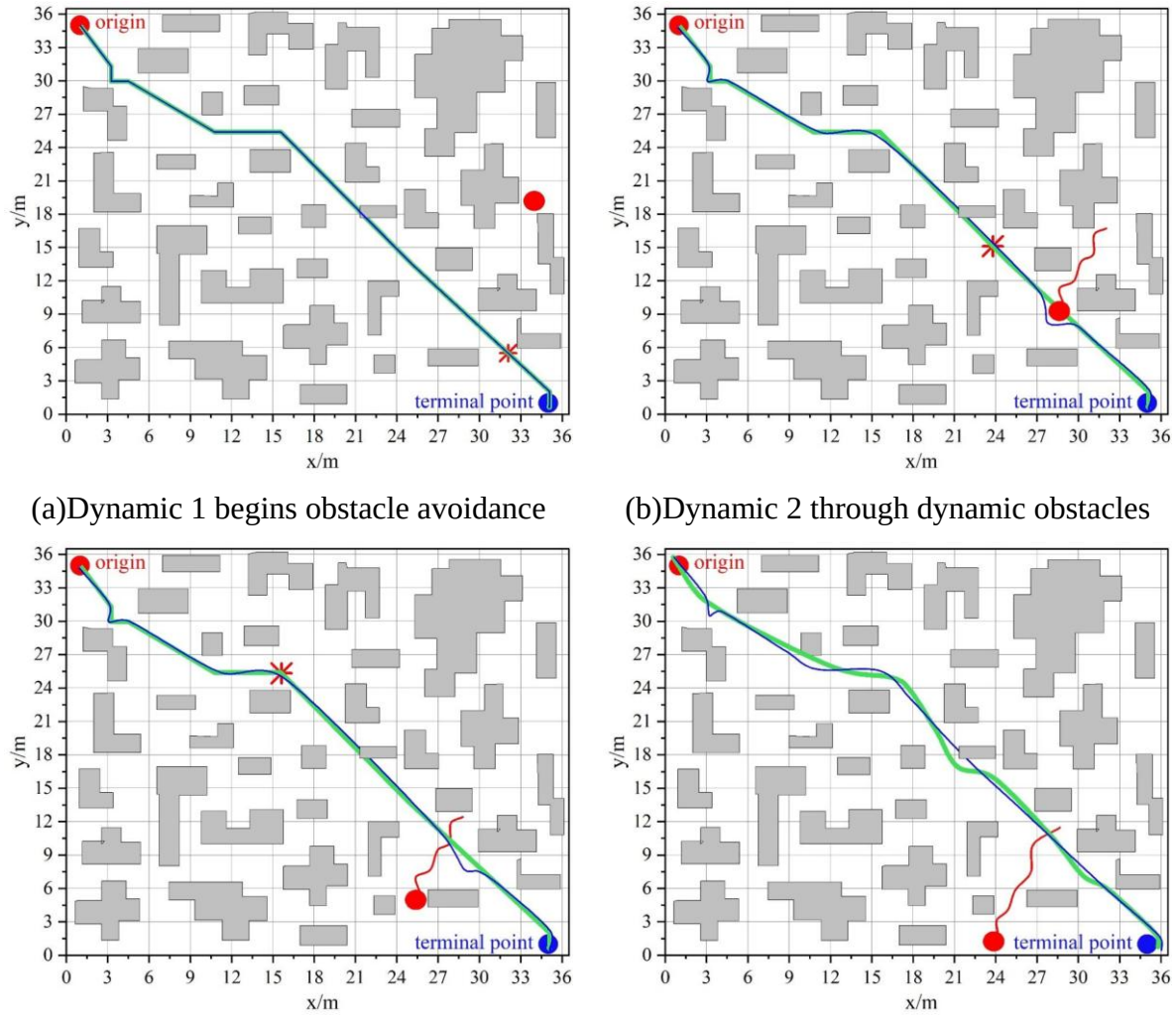

(a)Dynamic 1 begins obstacle avoidance (b)Dynamic 2 through dynamic obstacles

(c) Dynamic 3 through static obstacles (d) Dynamic 4 reaches the target point

Figure 6: Dynamic obstacle avoidance path planning results

The results of path planning with the introduction of random obstacles are shown in Fig. 7, where (a) ~ (c) represent 1~3 random obstacles, respectively. Through observation, it can be concluded that with the increase of the number of obstacles, the path length and the running time are increased, which is consistent with the actual situation.

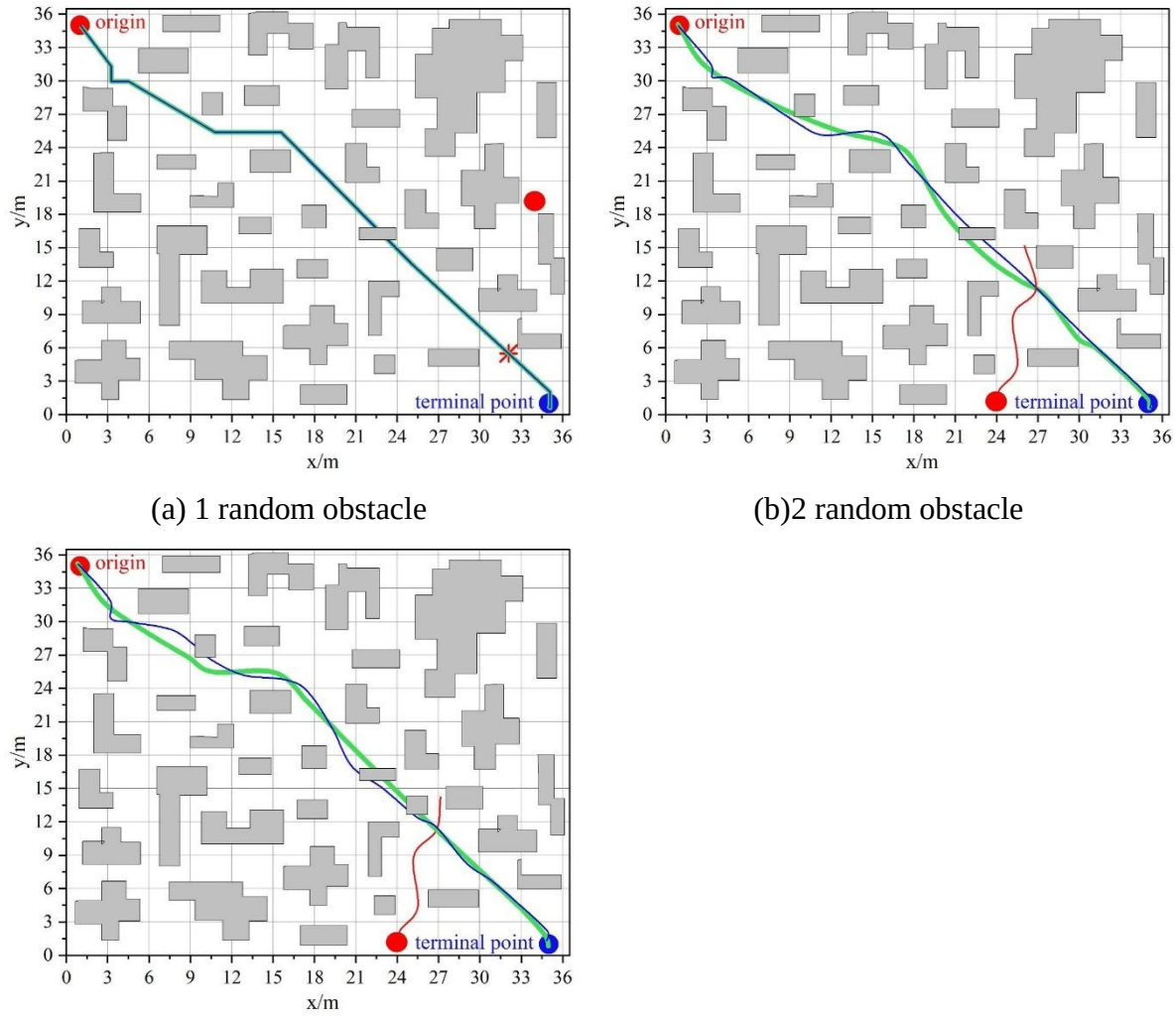

(a) 1 random obstacle

(b)2 random obstacle

(c)3 random obstacle

Figure 7: Path Planning Results with Random Obstacle

4 Conclusion

In order to realize the dynamic control of the transmission and transformation crane operation process, this paper firstly introduces the application model of digital twin technology in the crane operation process, and then utilizes the improved YOLOv5 model to identify the crane operation process and draws the fence map based on the point cloud data; and then combines with the improved A* algorithm to plan the paths of the transmission and transformation crane operation process.

In this paper, the improved YOLOv5 model can realize the violation detection of the transmission and transformation crane operation process, and the model has better detection results for targets such as operators, lifting booms and safety signs, as well as violation determination results, with an accuracy rate of more than 95%.

The improved A* algorithm runs faster and generates smoother paths, and it can plan the global path in a shorter time, so that the turning angle, the number of turns and the average number of search nodes of the transmission and transformation crane operation process are significantly reduced by 77.19%, 40% and 39.2%, and it can satisfy the demand for global path planning in the operation process of the transmission and transformation crane.

About the Author

Yi Zhou, graduated from Beijing Mechanical and Electrical University in 2007. is currently working at Beiiing Electric Power Transmission and Transformation Engineering Company, mainly engaged in electric power construction.

Haitao Jiang, graduated from Nanjing University of Science and Technology in 2015, currently working at State Grid Corporation of China's Ultra High Voltage Construction Branch, mainly engaged in power construction management work.

Ming Song, graduated from Shandong University of Technology in 1999 and is currently employed at the State Grid Corporation of China's Ultra High Voltage Construction Branch, where he specializes in power infrastructure management.

Kangwei Li, graduated from Hefei University of Technology in 2007, currently working at State Grid Corporation of China's Ultra High Voltage Construction Branch, mainly engaged in power construction management work.

Hua Wen graduated from Wuhan University in 2004. Currently, he/she is employed by Huada Tianyuan (Beijing) Technology Co., Ltd., mainly engaged in the digital and intelligent construction work of power grid infrastructure.

References

[1] Liu, J., Zhu, G., Xia, T., Xu, Z., Yang, Z., Zhou, L., ... & Lan, G. (2025). Key Technology for Hoisting and Construction of Node Frame Beams in Ultra-high Voltage Substations. International Core Journal of Engineering, 11(6), 56-64.

[2] Qiu, H., Wu, F., Chen, W., Liu, R., & Wang, C. (2024, March). Research on Steel Cage Hoisting Equipment in Electric Power Construction. In Journal of Physics: Conference Series (Vol. 2731, No. 1, p. 012030). IOP Publishing.

[3] Wang, Y. (2022). Research on Operation Safety of Power Transmission and Transformation Equipment in Wind Power Plant. International Journal of Frontiers in Engineering Technology, 4(6).

[4] Wu, C., Jia, P., Yu, X., Guan, J., Deng, J., & Cheng, H. (2022). Function orientation and typical application scenarios of the Internet of Things construction for power transmission and transformation equipment. Energy Reports, 8, 109-116.

[5] Priyono, P., Alihudien, A., & Fiendyo, H. (2025). REVIEW STUDY OF FOUNDATION STRUCTURE OF BELAWAN MEDAN CRANE ELECTRIFICATION SUBSTATION BUILDING REGARDING BEARING CAPACITY AND SETTLEMENT. Jurnal Pensil: Pendidikan Teknik Sipil, 14(3), 508-517.

[6] Milazzo, M. F., Ancione, G., & Consolo, G. (2021). Human factors modelling approach: Application to a safety device supporting crane operations in major hazard industries. Sustainability, 13(4), 2304.

[7] Peng, L., Man, S. S., Chung, H. T., Chan, A. H. S., & Zhang, Z. (2025). Prospective Workers' Perceptions of Crane Operation Risks: Using a Pairwise Comparison. Journal of Construction Engineering and Management, 151(7), 05025001.

[8] Wang, H., Yang, Q., Liu, Q., Zhao, C., & Zhou, W. (2024). Automatic Planning for Cable Crane Operations in Concrete Dam Construction. Journal of Construction Engineering and Management, 150(12), 04024177.

[9] Fakhri, A. B., Mohammed, S. L., Khan, I., Sadiq, A. S., Alkazemi, B., Pillai, P., & Choi, B. J. (2021). Industry 4.0: Architecture and equipment revolution. Comput. Mater. Continua, 66(2), 1175-1194.

[10] Dou, K., Li, J., Liu, J., Li, Q., & Zhou, Y. (2025). Configuration Study on Production Equipment Operation Management and Control Performance in Industrial Internet Environment. Sustainability, 17(21), 9890.

[11] He, B., & Bai, K. J. (2021). Digital twin-based sustainable intelligent manufacturing: a review. Advances in Manufacturing, 9(1), 1-21.

[12] Lai, X., Wang, S., Guo, Z., Zhang, C., Sun, W., & Song, X. (2021). Designing a shape–performance integrated digital twin based on multiple models and dynamic data: a boom crane example. Journal of Mechanical Design, 143(7), 071703.

[13] Jiang, W., Ding, L., & Zhou, C. (2022). Digital twin: Stability analysis for tower crane hoisting safety with a scale model. Automation in Construction, 138, 104257.

[14] Szpytko, J., & Salgado Duarte, Y. (2021). A digital twins concept model for integrated maintenance: a case study for crane operation. Journal of Intelligent Manufacturing, 32(7), 1863-1881.

[15] Ma, F., Jin, R., Zhao, P., Zhe, H., Li, D., & Li, W. (2025, November). High-precision safety monitoring technology for crane operation in substation based on YOLO model and stereo vision. In International Conference on Wireless, Optical Communication, and Information Engineering (WOCIE 2025) (Vol. 13973, pp. 172-180). SPIE.

[16] Zhidchenko, V., Malysheva, I., Handroos, H., & Kovartsev, A. (2018, September). Faster than real-time simulation of mobile crane dynamics using digital twin concept. In Journal of Physics: Conference Series (Vol. 1096, No. 1, p. 012071). IOP Publishing.

[17] Tu, X., Autiosalo, J., Jadid, A., Tammi, K., & Klinker, G. (2021). A mixed reality interface for a digital twin based crane. Applied Sciences, 11(20), 9480.

[18] Hussain, M., Ye, Z., Chi, H. L., & Hsu, S. C. (2024). Predicting degraded lifting capacity of aging tower cranes: A digital twin-driven approach. Advanced Engineering Informatics, 59, 102310.

[19] Yang, C., Yu, H., Zheng, Y., Feng, L., Ala-Laurinaho, R., & Tammi, K. (2025). A digital twin-driven industrial context-aware system: A case study of overhead crane operation. Journal of manufacturing systems, 78, 394-409.

[20] Farrage, A., Takahashi, H., Terauchi, K., Sasai, S., Sakurai, H., Okubo, M., & Uchiyama, N. (2023). Trajectory generation of rotary cranes based on A* algorithm and time-optimization for obstacle avoidance and load-sway suppression. Mechatronics, 94, 103025.

[21] Bagheri, S. M., Taghaddos, H., Mousaei, A., Shahnavaz, F., & Hermann, U. (2021). An A-Star algorithm for semi-optimization of crane location and configuration in modular construction. Automation in Construction, 121, 103447.

[22] Li, D., Shi, X., & Dai, M. (2023, November). An improved path planning algorithm based on a* algorithm. In International Conference on Computer Engineering and Networks (pp. 187-196). Singapore: Springer Nature Singapore.

[23] Wang, H., Lou, S., Jing, J., Wang, Y., Liu, W., & Liu, T. (2022). The EBS-A* algorithm: An improved A* algorithm for path planning. PloS one, 17(2), e0263841.

[24] Niu, C., Li, A., Huang, X., Li, W., & Xu, C. (2021). Research on global dynamic path planning method based on improved A∗ algorithm. Mathematical Problems in Engineering, 2021(1), 4977041.